Online supporting information:

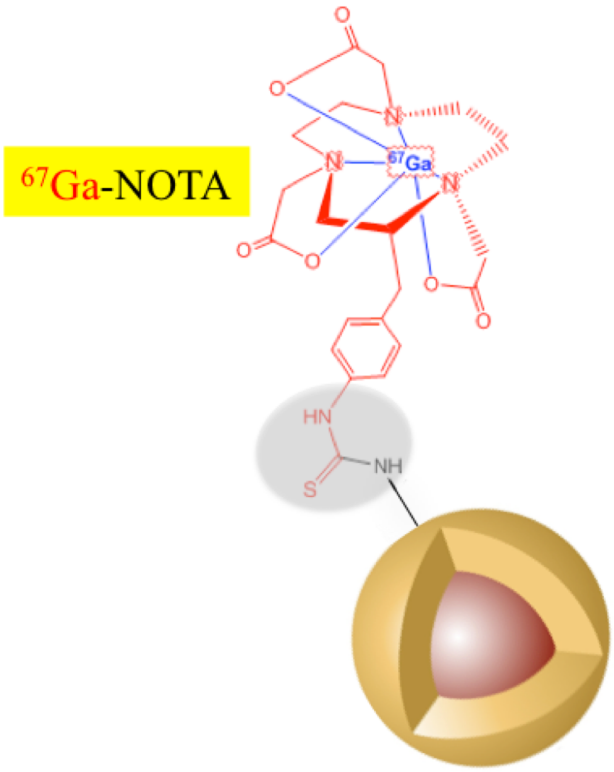

Fig. S1 Schematic showing radiolabeling of the amine groups on the surface of the NPs with ^{67}Ga using NOTA chelator.

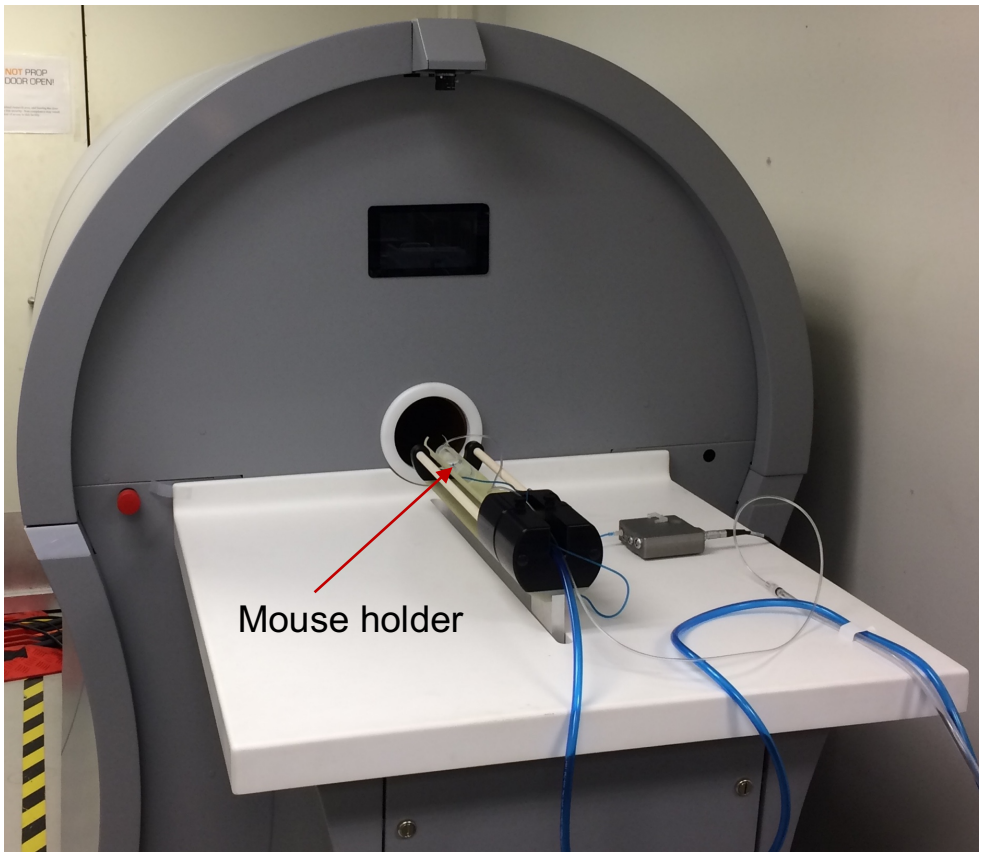

Fig. S2 Magnetic Particle Imaging (MPI) scanner used for whole mice imaging.

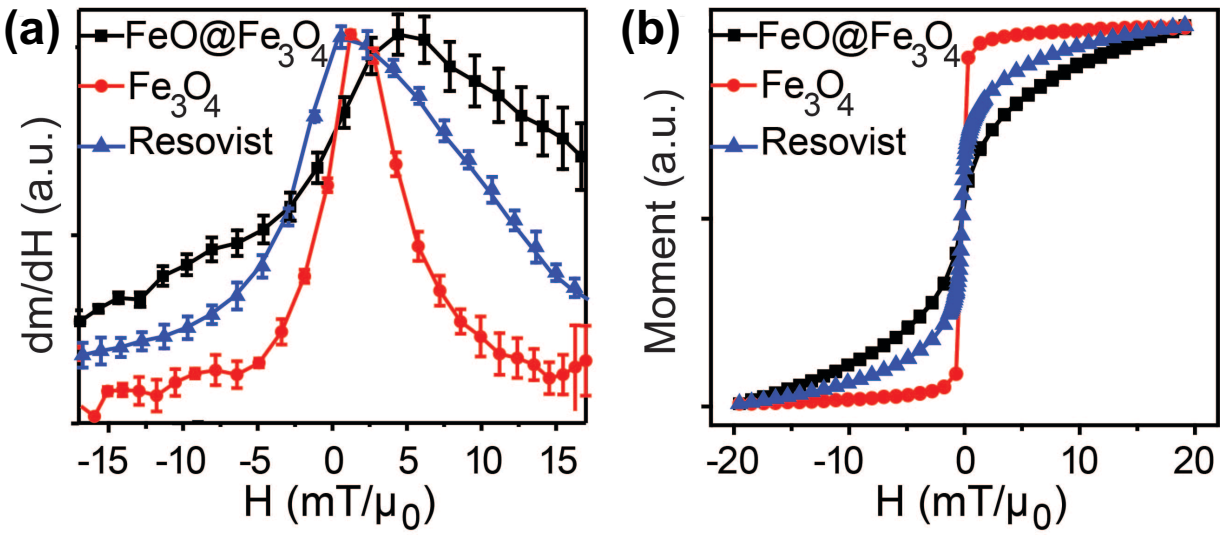

Fig. S3 Nanoparticles d*m*/d*H* measured in a MPS, and *m*-*H* plots obtained by dc measurements in a VSM showed narrower FWHM (higher MPI resolution) and smallest saturation fields for single crystalline magnetite NPs (d_C~27nm) in comparison with Wüstite/magnetite core/shell NPs and a commercially provided nanoparticles formulation, Resovist®.[21]-Reproduced by permission of The Royal Society of Chemistry.

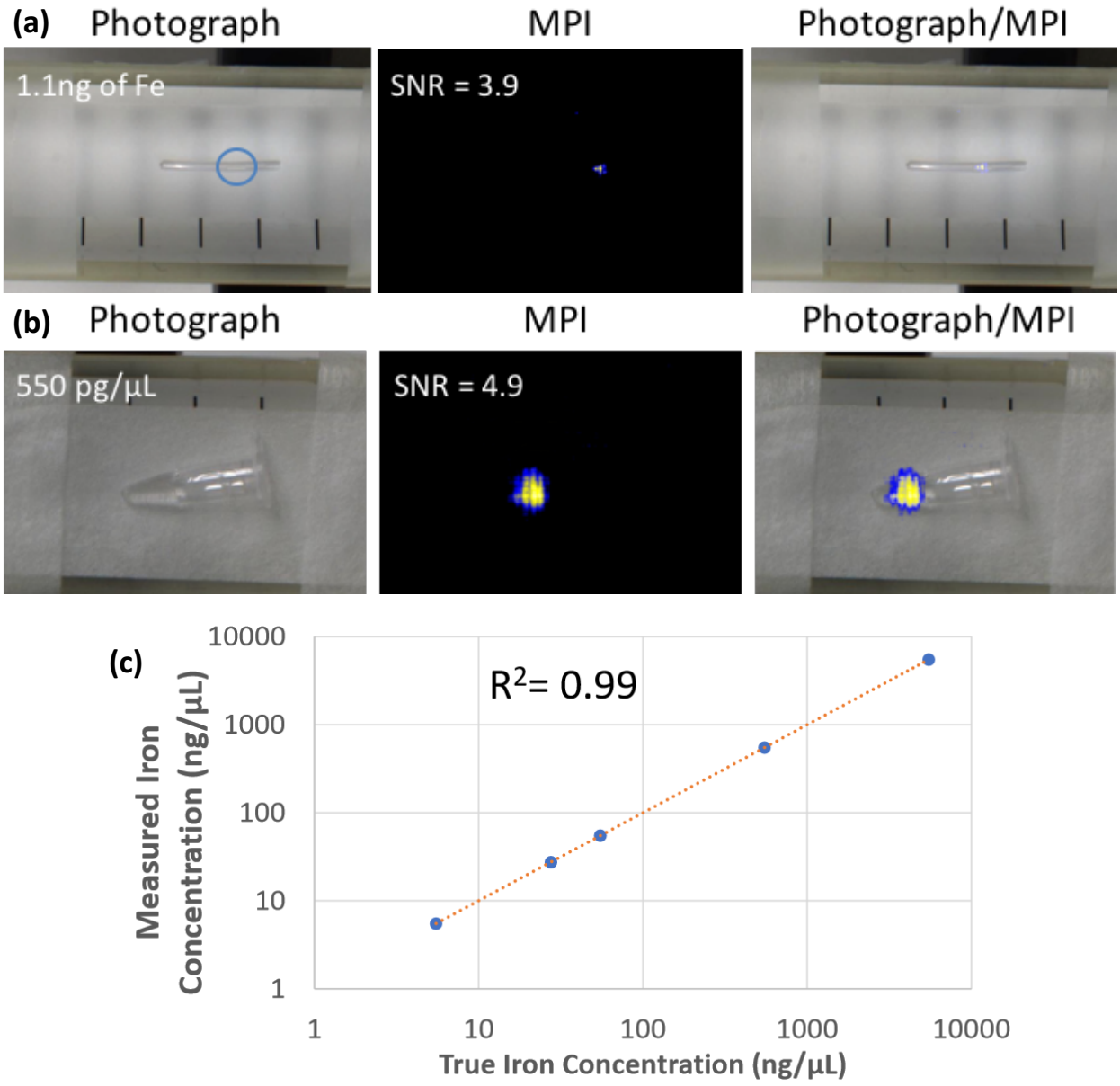

Fig. S4 High sensitivity of the MPI scanner to our optimized contrast agents: (a) High sensitivity imaging showing detection of less than 2-3µL of NPs solution (shown by blue color circle) containing 1.1ng of iron (SNR=3.9). (b) Detection of about 200µL of NPs solution with a concentration of 550pg Fe/µL, with a signal-to-noise (SNR) ratio of 4.9. The images were prepared without any filtering. (c) Linear variation of the MPI signal intensity with concentration of the nanoparticles, ranging from less than 10ng Fe/µL to about 10,000ng Fe/µL.

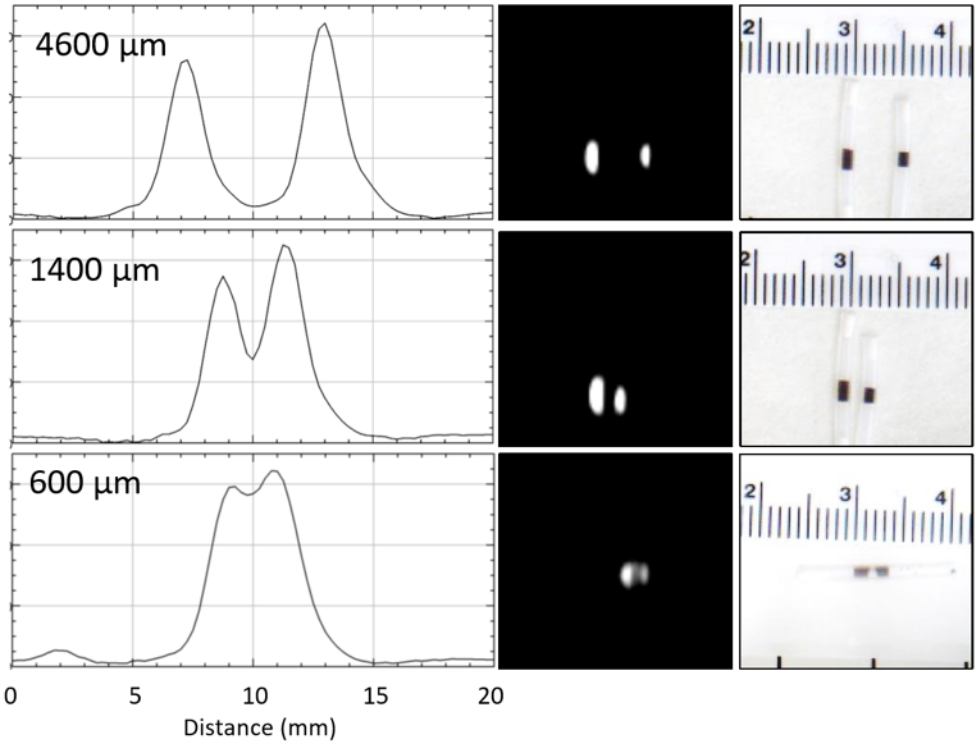

Fig. S5 *In vitro* evaluation of achievable spatial resolution using our optimized MPI contrast agents and the MPI scanner used for this study. NPs solutions (1-2µL each, 1.1mg/mL) were injected into tubing and placed at different distances (~ 4600, 1400 and 600µm) relative to each other for imaging. Results show that MPI scanner could distinguish these separate volumes of NPs, even when their approximate distance was adjusted to ~600 µm. The images were prepared without any filtering. The profile was prepared based on the center point of the two adjacent samples and is shown as inverted along the x-axis. Sample distances were measured using the average number of pixels separating the two samples. Note that when sample are very close (*i.e.* less than 1mm distance) their distance is variable due to the shape of the air bubble trapped between them, which adds some error to the measurement. We used the closest edges of the two adjacent samples to estimate their distance.

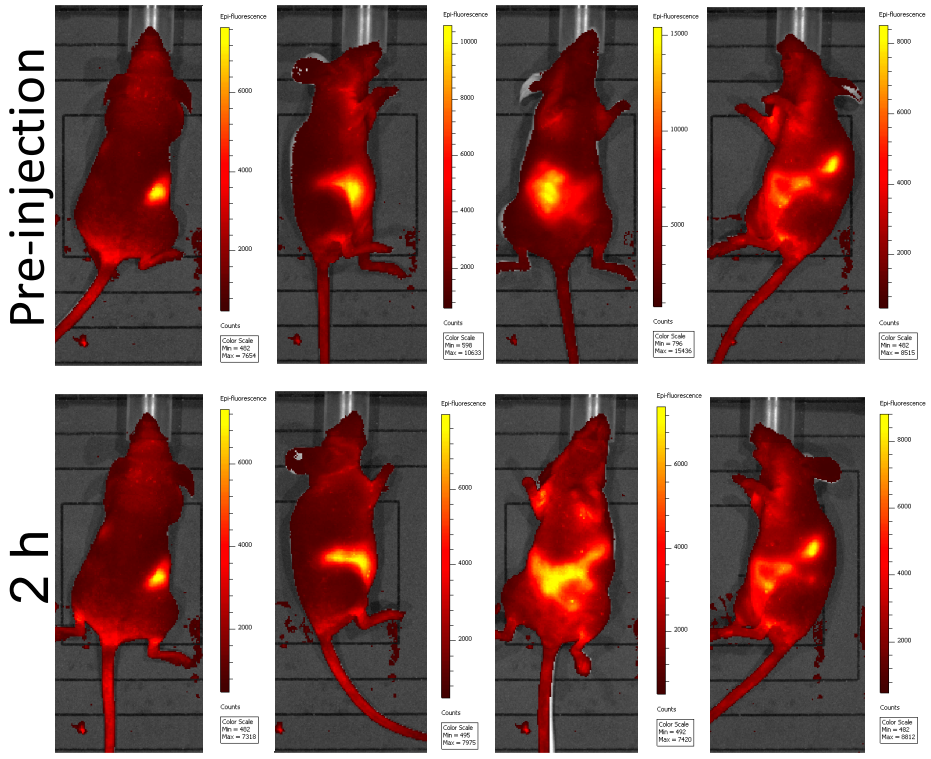

Fig. S6 Fluorescent images of a control mouse (anesthetized) with brain cancer xenograft, at different angles, before and 2 hours after injection of PBS (1x). The bright spots are related to innate autofluorescence of the mice and have a much weaker signal intensities compared with fluorescent signals observed in mice after injection of Cy5.5 labeled NPs, shown in Figs. 3 and S7-S10.

(a)

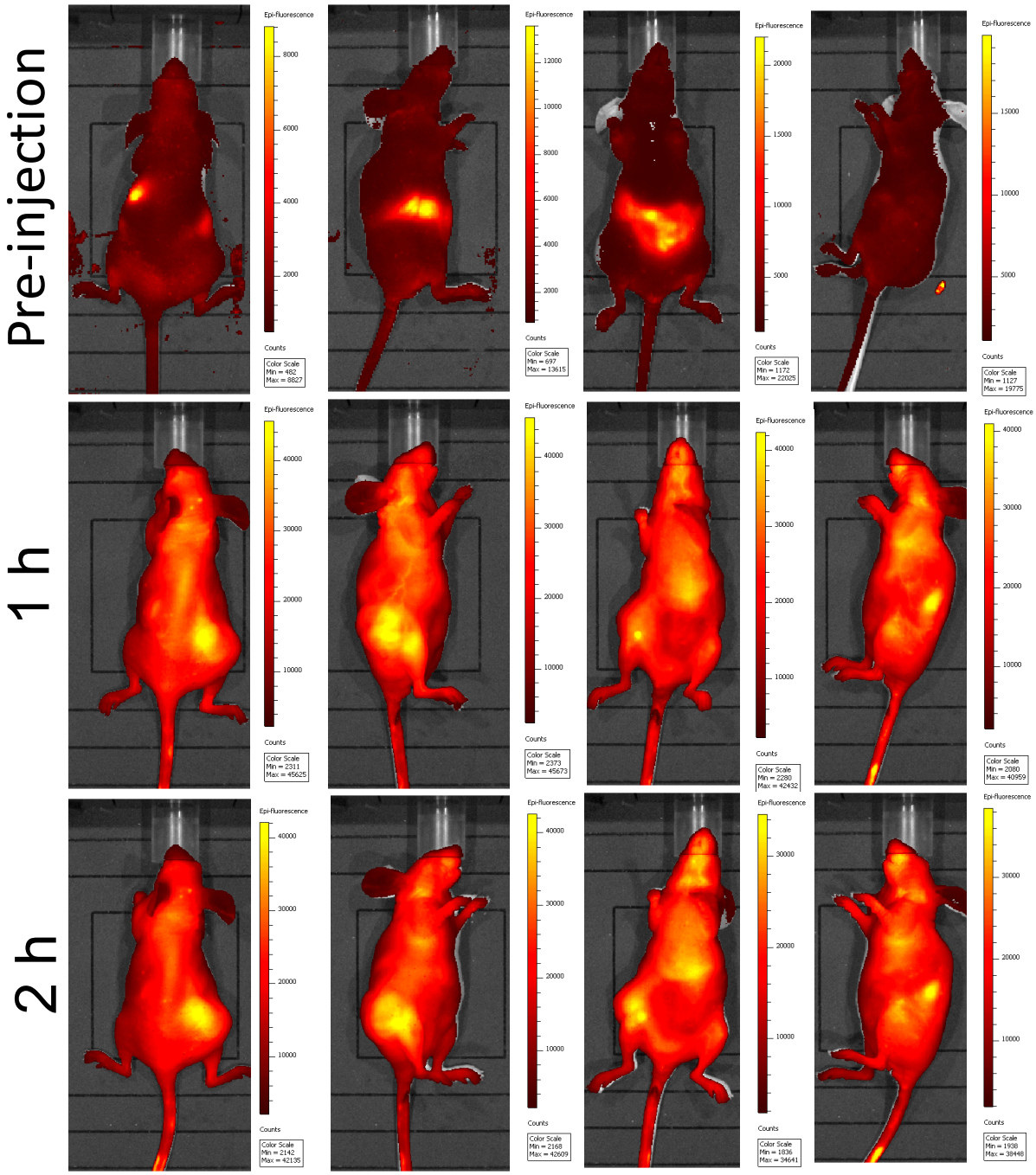

Fig. S7 Continued.

(b)

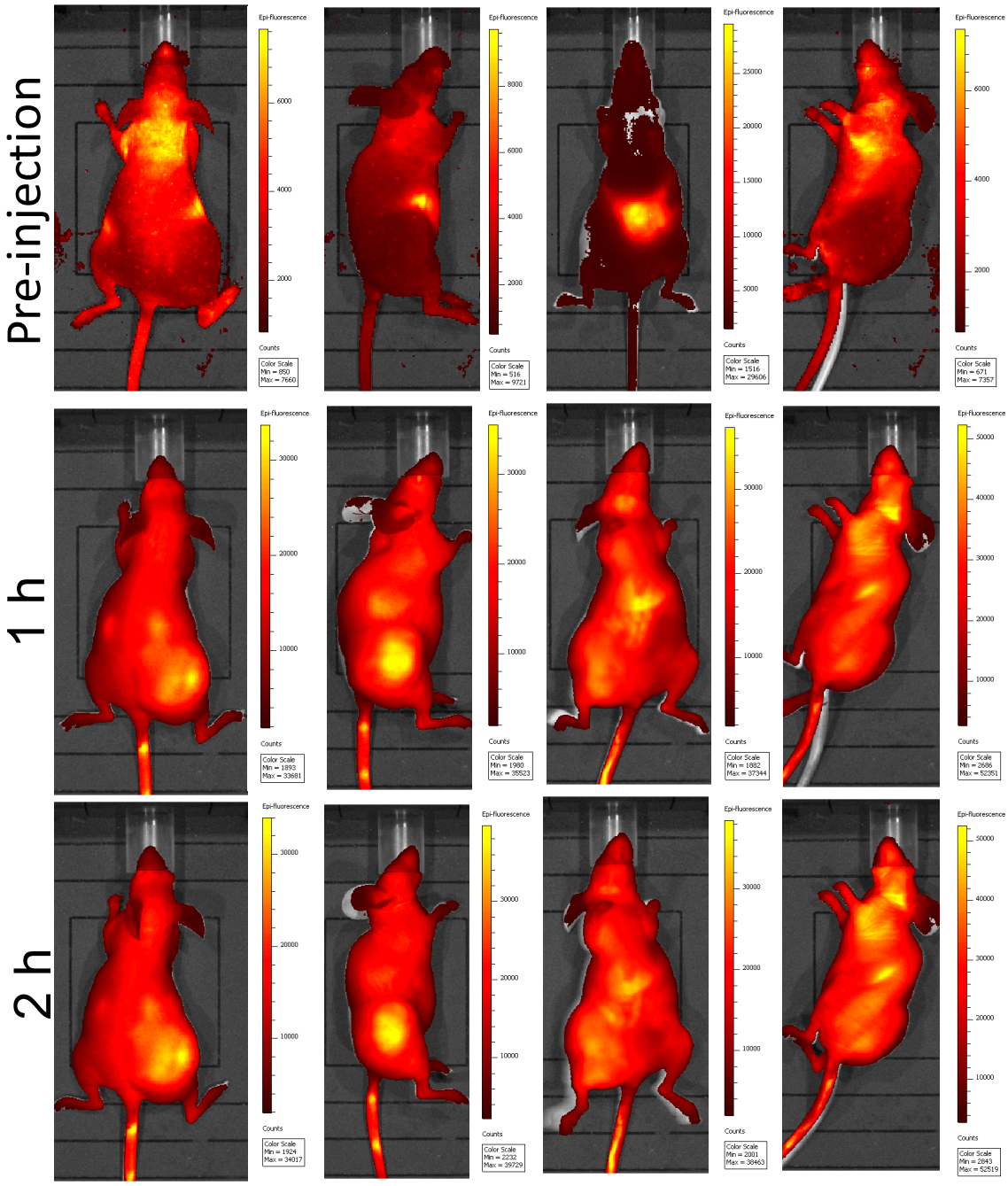

Fig. S7 Continued.

(c)

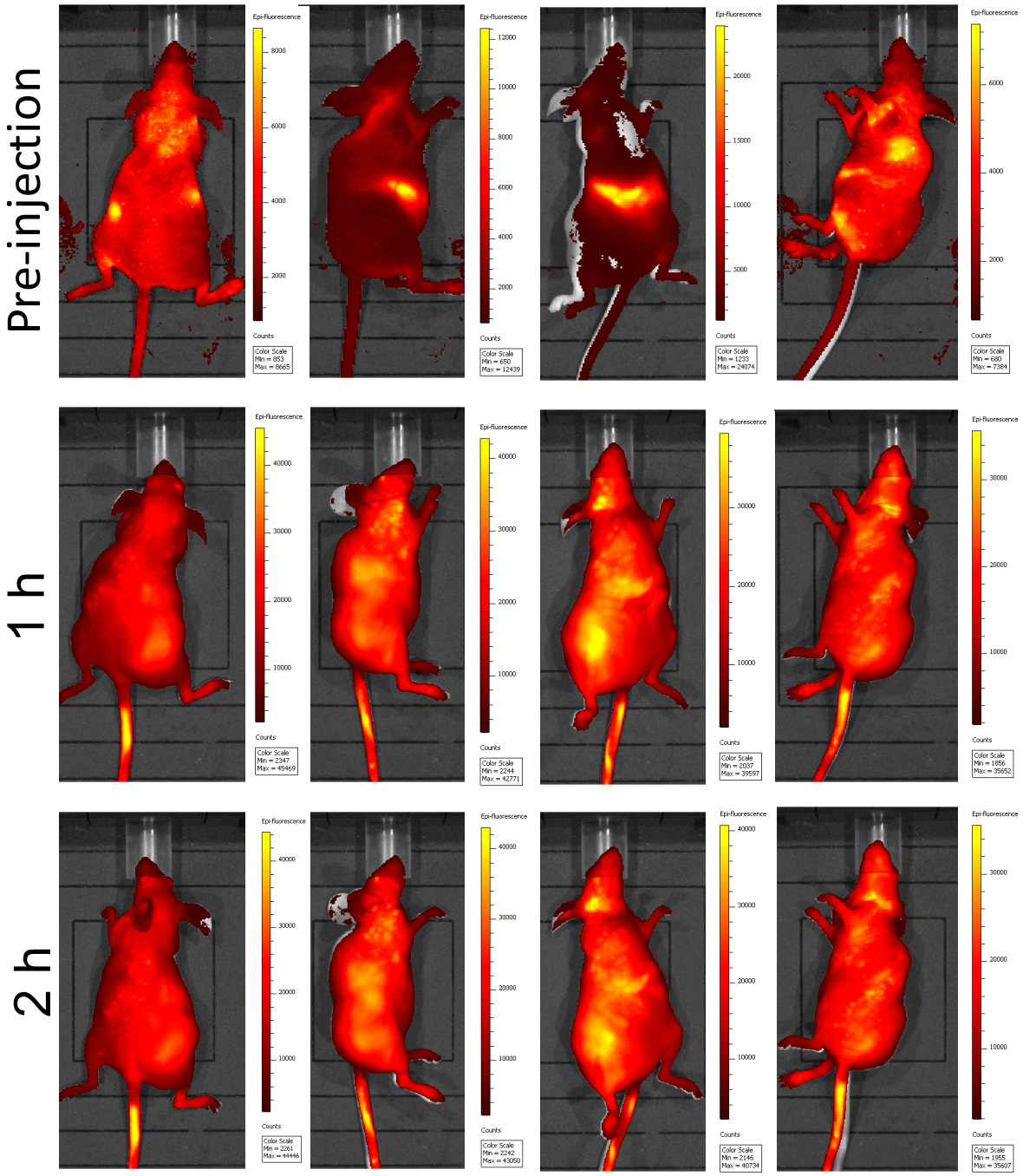

Fig. S7 NIRF images of the mice injected with Cy5.5-Lactoferrin conjugated NPs, with (a) and without (b) a permanent magnet placed adjacent to the tumor xenograft on the right side flank, compared with mice injected with Cy5.5-labeled NPs, without using lactoferrin and magnetic targeting (c). Three mice were used for each condition and pre-injection and post-injection (1 and 2h) images were captured from four different mice positions to show NPs accumulation in tumors clearly (see additional mice images in Figs. S9-S11).

(a)

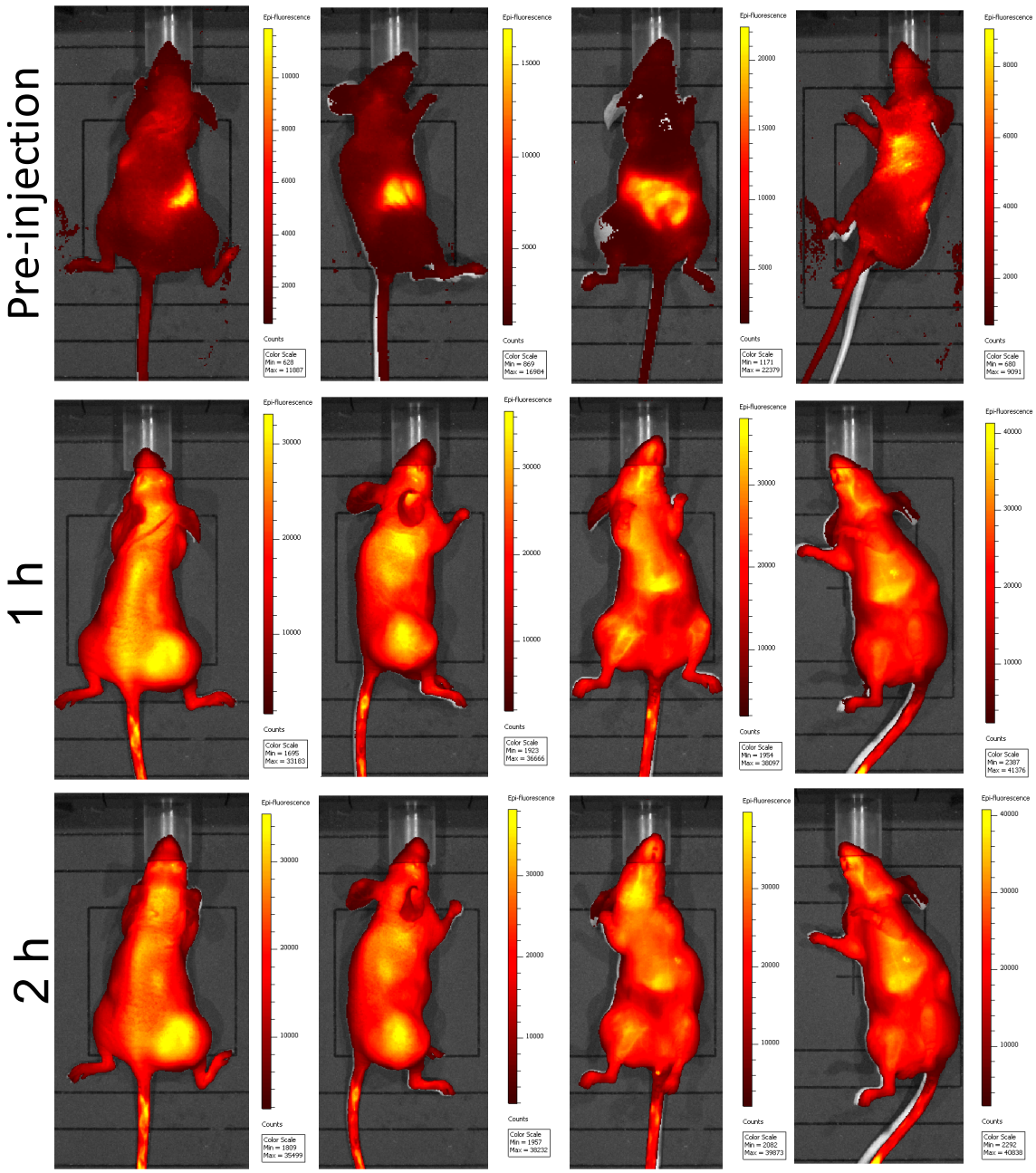

Fig. S8 Continued.

(b)

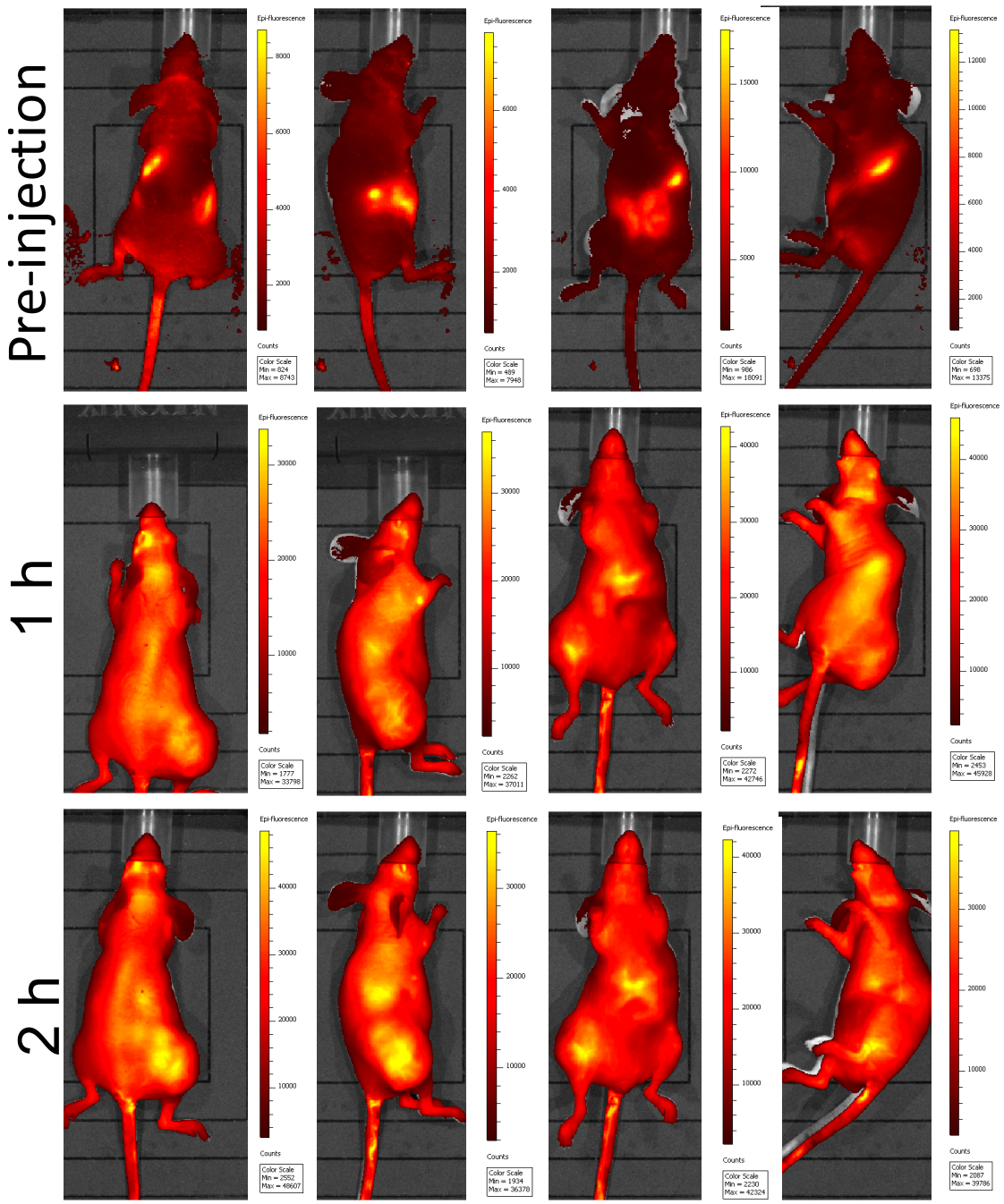

Fig. S8 IVIS images of the other two mice injected with Cy5.5-Lactoferrin conjugated NPs, with a magnet placed adjacent to the tumor xenograft on the right side flank.

(a)

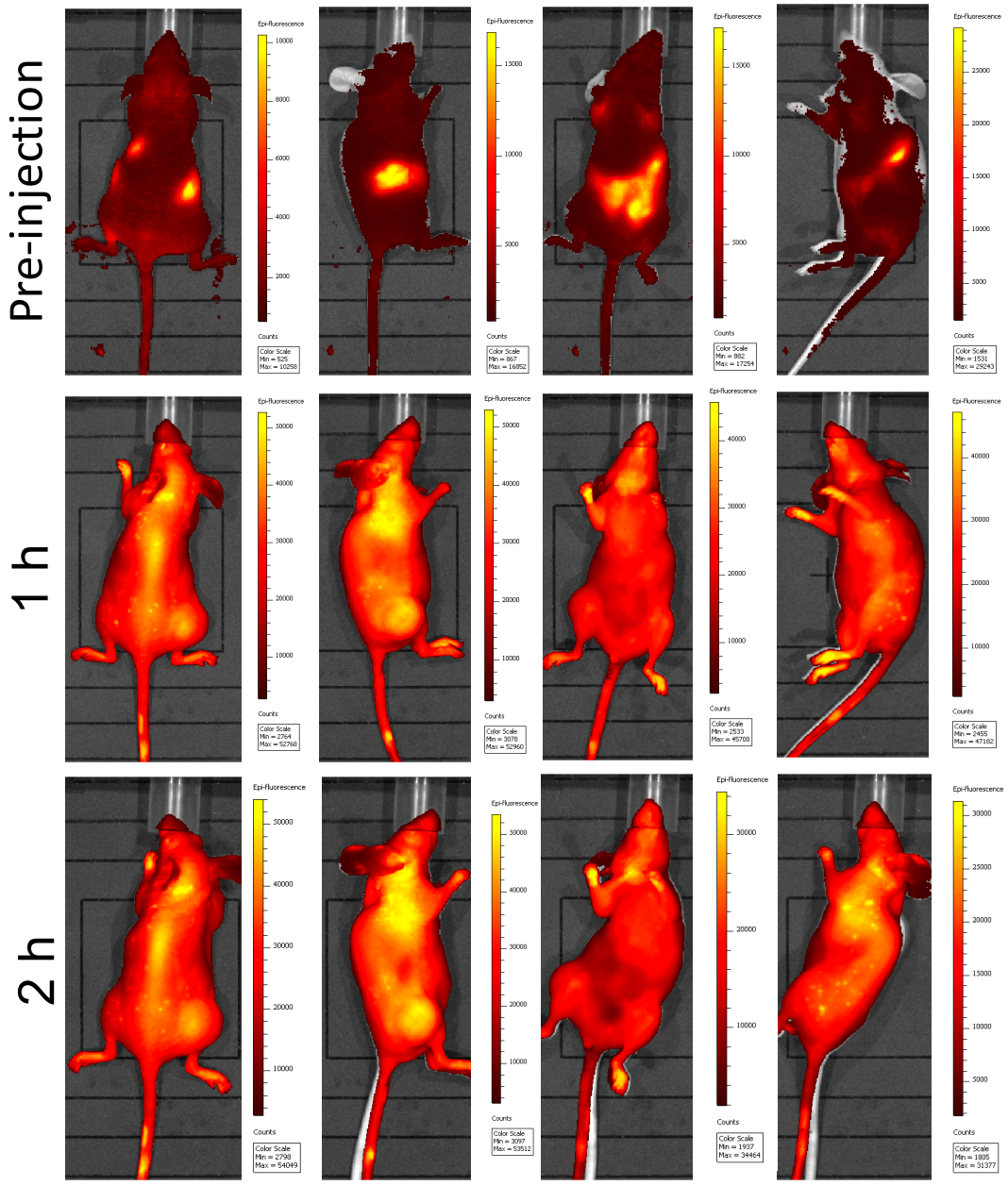

Fig. S9 Continued.

(b)

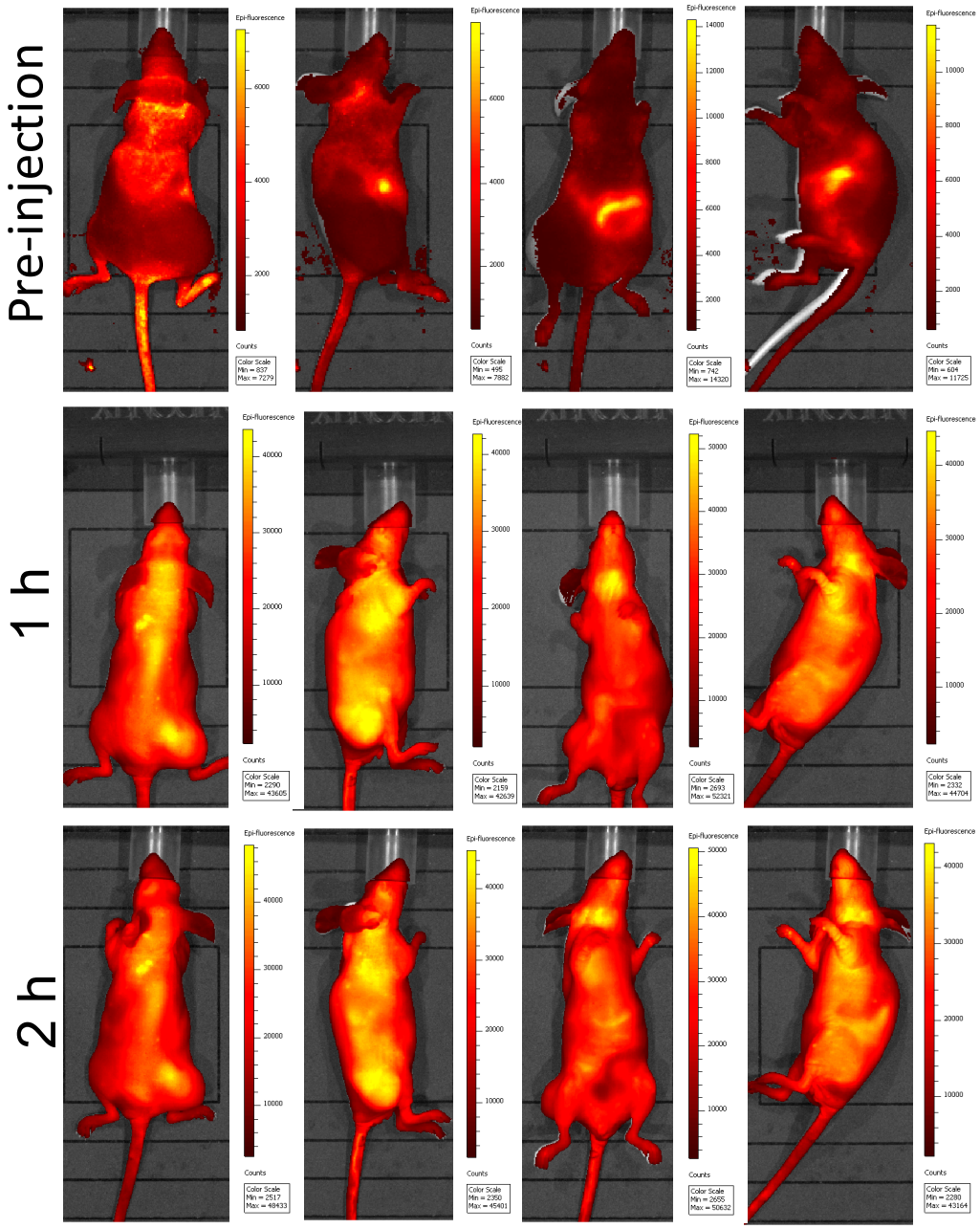

Fig. S9 IVIS images of the other two mice injected with Cy5.5-Lactoferrin conjugated NPs, without using magnetic targeting.

(a)

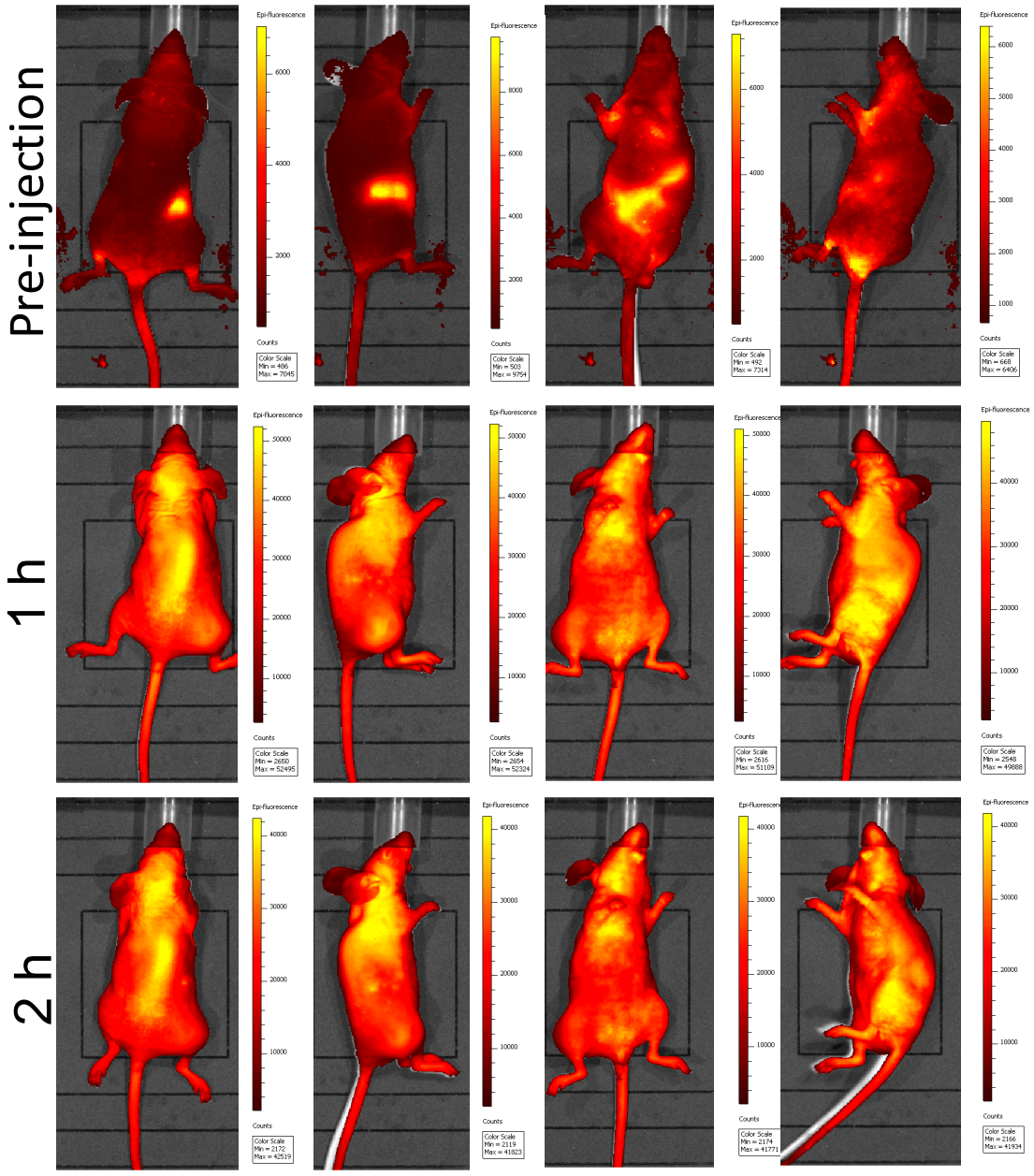

Fig. S10 Continued.

(b)

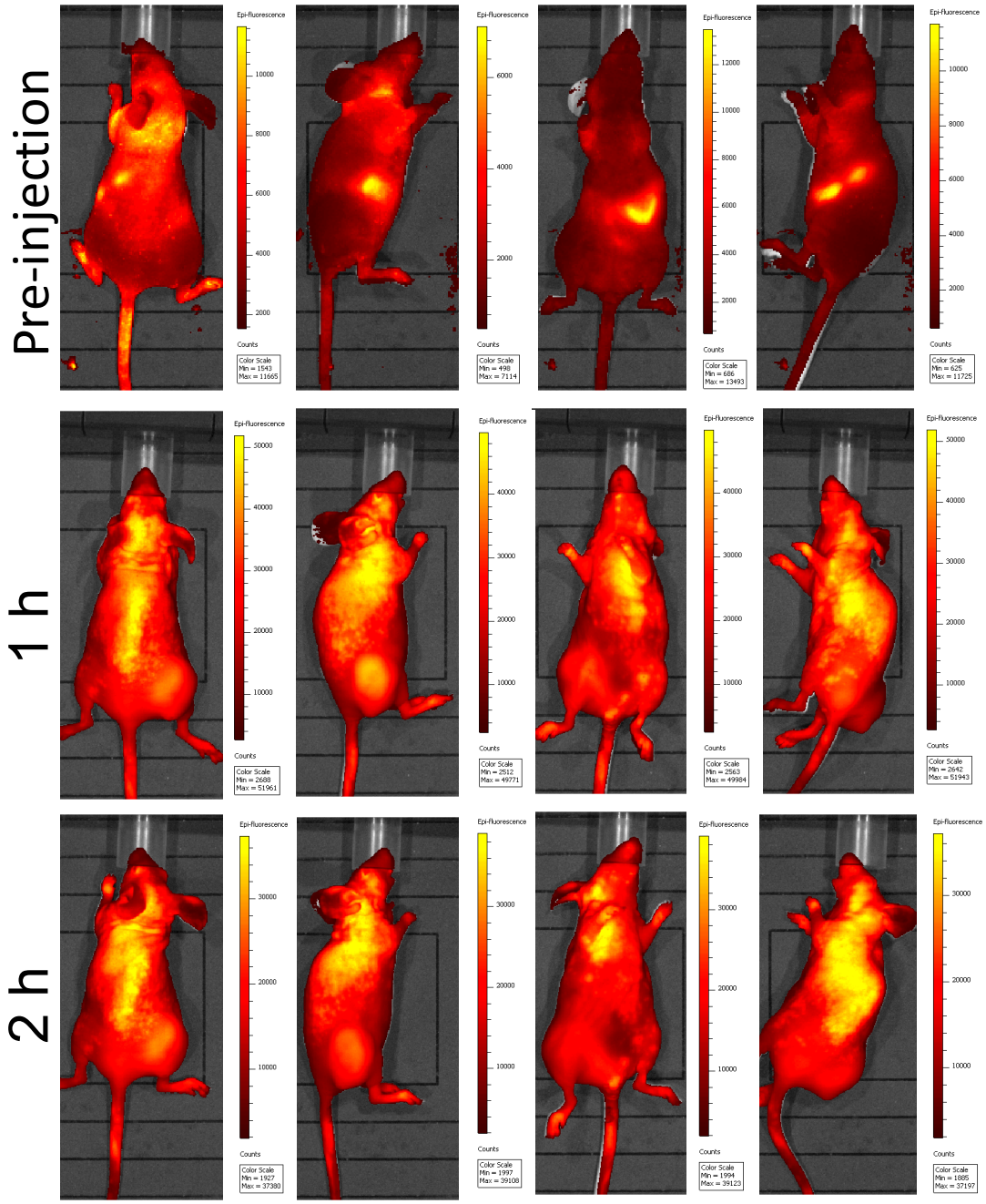

Fig. S10 IVIS images of the other two mice injected with Cy5.5-labeled NPs, without using lactoferrin and magnetic targeting.

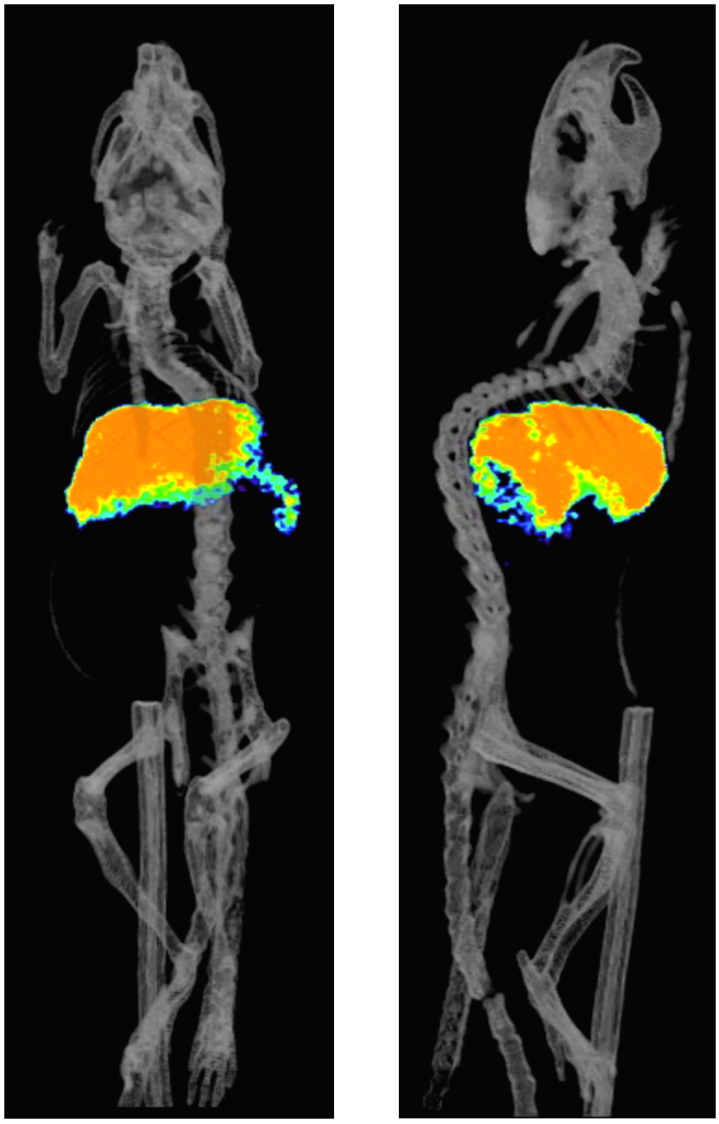

Fig. S11 SPECT/CT image of a mouse showing the biodistribution of the ^{67}Ga-NOTA-labeled MPI contrast agents in mice, 4h after tail vein injection. NPs were only accumulated in liver and spleen with no trace of NPs observed in kidneys or other organs (also see biodistribution results in Fig. S12 and Supporting Videos 4 and 5).

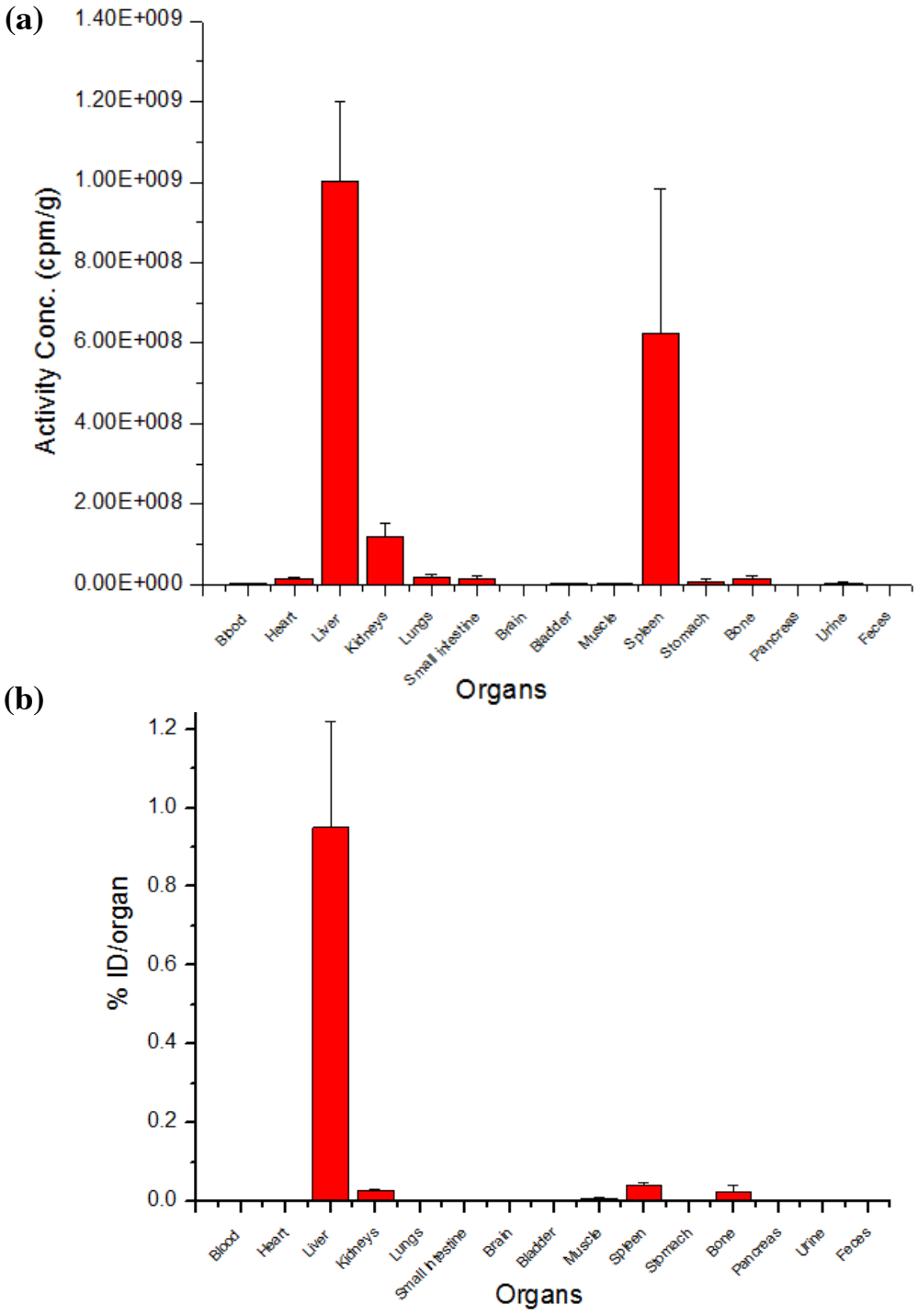

Fig. S12 Continued.

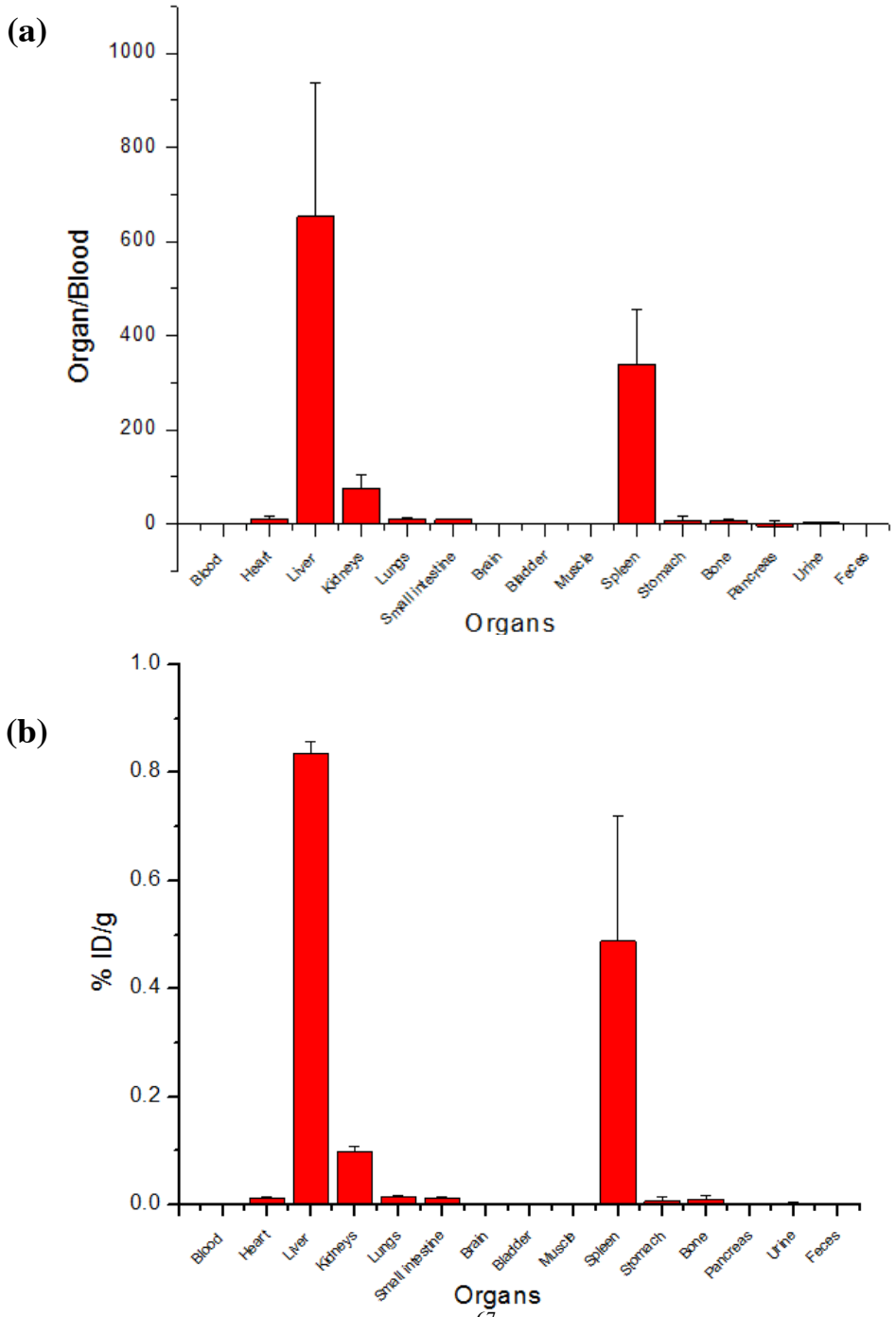

Fig. S12 Quantitative biodistribution of the ^{67}Ga-NOTA-labeled MPI nanoparticles in mice (n=3), 4h after tail vein injection. All graphs confirm that NPs were mainly accumulated in liver and spleen. The results are shown based on (a) radiation activity observed in each organ, (b) percentage of the injected NPs in each organ, (c) percentage of the NPs in each organ divided by the dosage observed in the blood and (d) percentage of the NPs per gram of organs.